Research Article

Journal of MASS SPECTROMETRY

Received: 09 December 2009 Accepted: 09 May 2010

(www.interscience.com) DOI 10.1002/jms.1765

A TPD-MS study of the interaction of coumarins and their heterocyclic derivatives with a surface of fumed silica and nanosized oxides CeO_2/SiO_2, TiO_2/SiO_2, Al_2O_3/SiO_2

Kostiantyn Kulyk,[a] Valentyna Ishchenko,[b] Borys Palyanytsya,[c]
Volodymyr Khylya,[b] Mykola Borysenko[a] and Tetiana Kulyk[c]*

The interactions between coumarins and the surface of fumed SiO_2, CeO_2/SiO_2, TiO_2/SiO_2 and Al_2O_3/SiO_2 were assessed by means of temperature-programed desorption mass spectrometry. The different stages of the thermolysis of coumarin were identified and an analysis of the underlying reactions was performed. The kinetic parameters of the involved reactions were thus obtained. The decomposition of thiazolyl-substituted coumarins was found to proceed through a 'thiazole–thiazine' ring expansion in the adsorbed state. A linear correlation between the sigma constants ($\Sigma\sigma$) of the coumarin substituents and the activation energy of CO_2 formation was obtained. Copyright © 2010 John Wiley & Sons, Ltd.

Keywords: TPD-MS; coumarins; fumed silica; nanosized oxides; kinetic parameters

Introduction

The study of the thermal transformations of coumarins is of practical value due to the widespread application of these compounds as matrixes in matrix-assisted laser desorption and ionization mass spectrometry (MALDI MS). The derivatization properties of coumarins are intimately related to their acid–base properties, particularly to their ability to form hydrogen-bonded and donor–acceptor complexes with analyte molecules that have proton-donating or electron-donating groups. Another important though less reported aspect of the effectiveness of coumarins as MALDI MS matrixes is their pattern of thermal transformation. Some studies have been published[1–4] and models of ionization have been suggested such as those of disproportionational, polyphotonic and thermal ionization. It seems however evident that the mechanisms of ionization of molecules during MALDI MS tests have not been fully elucidated and need a further deep study in order to develop fundamental models. Therefore investigation of mechanisms of thermal reactions of coumarins by means of temperature-programed desorption mass spectrometry (TPD-MS) could be useful for the identification of the ionization mechanisms in MALDI MS and in surface-assisted laser desorption and ionization mass spectrometry (SALDI MS).[5] TPD-MS technique is widely used in surface chemistry for the study of adsorption and desorption processes, surface reactions and surface properties of various objects.[6–14]

Particularly a methodology should be developed to link empirical kinetic data such as global reaction rates, energies and entropies of activation to fundamental molecular structure features. An appropriate one seems to be the building of quantitative structure–activity relationships based on the linear free energy relationship (LFER) principle.[15] The LFER principle is based on the linear correlation of the logarithm of the rate constant (or equilibrium constant) of one reaction with the related sets of other reactions which differ from the first one by one-type changes in the reagent structures and experimental conditions. As it has been shown in previous works,[16–18] these correlations allow to describe quantitatively the changes in the reaction medium, substrate structure (Hammett equation[19,20] and Taft equation[21,22]) or reagent structure (Brønsted catalysis equation[23]). Such information could be obtained from the analysis of TPD-MS data. A review by Kraus[24] is specially devoted to the description of linear correlations of substrate reactivity in heterogeneous catalytic reactions.

With respect to the chosen adsorbate, their importance cannot be overemphasized. Coumarins are compounds derived from α-pyrone and are important biologically active phytogenous substances. A great value is specially attributed to synthetic, modified coumarins in which the nucleus is modified with heterocyclic groups. These groups are chosen for their biological activity and the final products find wide use as medicines[15] because of their good balance of high biological activity and low toxicity. This activity comprises many practical medicine

---

* Correspondence to: Tetiana Kulyk, Department of Amourphous and Structurally Ordered Oxides, Chuiko Institute of Surface Chemistry of National Academy of Sciences of Ukraine, 17 Generala Naumova Street, Kyiv 03164, Ukraine. E-mail: tanyakulyk@gala.net

a Department of Oxide Nanocomposites, Chuiko Institute of Surface Chemistry of National Academy of Sciences of Ukraine, 17 Generala Naumova Street, Kyiv 03164, Ukraine

b Department of Organic Chemistry, Taras Shevchenko Kyiv National University, 64 Volodymyrska Street, Kyiv 01033, Ukraine

c Department of Amourphous and Structurally Ordered Oxides, Chuiko Institute of Surface Chemistry of National Academy of Sciences of Ukraine, 17 Generala Naumova Street, Kyiv 03164, Ukraine

therapeutic effects such as blood anticoagulation, capillary tubes strengthening, hypotension, antispasmodic, anti-inflammatory and cholagogue effects.[25,26]

The specific interest on the coumarin–silica system follows the venue on modern medical drugs. The development of complex drugs based on biologically active compounds and nanosized silica has drawn much interest because of their demonstrated longer therapeutic effect.[27] For example, some derivatives of another natural oxygen heterocycles γ-pyrones and chromones[28–30] and biologically active substituted cinnamic acids have been lately studied.[31,32] Despite the importance of the gathered empirical evidence, the development of complex drugs demands more detailed information about the interactions in the adsorbed state, the structure of surface complexes and their mechanism of formation. Such information could be obtained from the analysis of TPD-MS data.[31,32] Of special interest would be the application of this technique to the elucidation of the binding mechanisms of coumarins on the silica surface.

This work focuses on the study of some of the most used coumarin drugs, namely the hydroxy- and methoxy-substituted coumarins and the synthetic thiazole and benzothiazole derivatives of α-pyrone.

Experimental

Materials

Powdery fumed silica ($S_a = 300\,m^2g^{-1}$) with a specific surface area of $300\,m^2g^{-1}$, fumed Al_2O_3/SiO_2 ($S_a = 207\,m^2g^{-1}$, 1.2% Al_2O_3, amount of aluminum atoms in surface layer 6.2%) and fumed TiO_2/SiO_2 ($S_a = 156\,m^2g^{-1}$, 14% TiO_2, amount of titanium atoms in surface layer 7.8%) were supplied by the Research and Experimental plant of the Chuiko Institute of Surface Chemistry (Kalush, Ukraine). Nanocomposite CeO_2/SiO_2 ($S_a = 265\,m^2g^{-1}$, 6.6% CeO_2) was prepared using powdery fumed silica and acetylacetonate of cerium $[CH_3COCH{=}C(CH_3)O]_3Ce{\cdot}H_2O$ (Aldrich). Modification of silica with cerium acetylacetonate was performed by a liquid-phase method (with carbon tetrachloride as a solvent).[33]

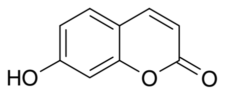

1

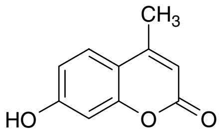

2

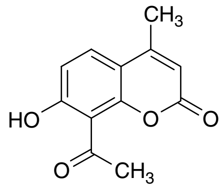

3

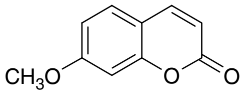

4

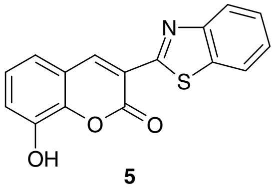

5

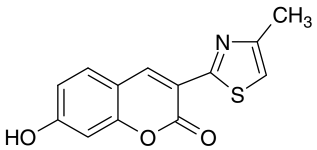

6

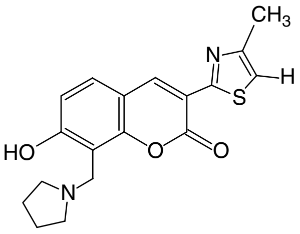

7

Coumarins **1–4** and 4-methylthiazole were supplied by Fluka. Coumarins **5–7** were synthesized at the Department of Organic Chemistry of Taras Shevchenko Kyiv National University. NMR spectral data. Coumarine **5**. (δ, ppm) 9.15–4-H (1H, s); 7.1–7.6–5-H (1H, m); 7.1–7.6–6-H (1H, m); 7.1–7.6–7-H (1H, m); 10.35–8H (1H, broadened s, OH). δ H (Het) 7.52 (2H, m, 4-H, 7-H), 7.20 (2H, m, 5-H, 6-H). Coumarine **6**. 8.85–4-H (1H, s); 7.81–5-H (1H, d, $J^3 = 8$); 6.64–6-H (1H, dd, $J^3 = 8$, $J^4 = 2.5$); 10.91–7-H (1H, broadened s, OH); 6.83–8H (1H, d, $J^4 = 2.5$). δ H (Het) 2.44 (3H, s, Me), 7.36 (1H, s, 5-H thiazole). Coumarine **7**. 8.73–4-H (1H, s); 6.80–5-H (1H, d, $J^3 = 9$); 7.44–6-H (1H, d, $J^3 = 9$); 4.23 – (8-CH_2); 1.92 (4H, m, $2CH_2$); 2.77 (4H, m, $2CH_2N$). δ H (Het) 2.52 (3H, s, Me), 7.01 (1H, s, 5-H thiazole). Samples of silica (SiO_2, CeO_2/SiO_2, Al_2O_3/SiO_2 and TiO_2/SiO_2) supported coumarin with loadings of 0.3, 0.4 and 0.6 mmol g^{-1} were obtained by impregnation. In a typical sample preparation session a portion (1 g) of fumed silica was gradually mixed with ethanol solution (25 ml) of coumarin. The sample was then aged at room temperature for 24 h and dried on air.

Temperature-programed desorption mass spectrometry

TPD-MS experiments were performed in an MKh-7304A monopole mass spectrometer (Electron, Sumy, Ukraine) with electron impact ionization, adapted for thermodesorption measurements. A typical test comprised placing a 20 mg sample on the bottom of a molybdenum-quartz ampoule (5.4 mm in diameter, a length of 20 cm and the volume 12 ml), evacuating to $\sim 5{\cdot}10^{-5}$ Pa at $\sim 20\,^\circ C$ and then heating at $0.15\,^\circ C\,s^{-1}$ from room temperature to $\sim 750\,^\circ C$. For all the samples, the sample vials were filled approximately 1/16 full, what helped (as it was shown in the works[8,10]) to limit interparticle-diffusion effects. The works[8,10,34–36] demonstrate that limiting sample volume along with the high vacuum should further limit readsorption and diffusion resistance. The volatile pyrolysis products passed through a high-vacuum valve into the ionization chamber of the mass spectrometer where they were ionized and fragmented by electron impact. After mass separation in the mass analyzer, the ion current due to desorption and thermolysis was amplified with a VEU-6 secondary-electron multiplier. The mass spectra were recorded and analyzed using a computer-based data acquisition and processing setup. The mass spectra were recorded within 1–210 amu. During each TPD-MS experiment, ~240 spectra were recorded. During a thermodesorption experiment the sample was heated slowly while keeping a high rate of evacuation of the volatile pyrolysis products. Diffusion effects can thus be neglected and the intensity of the ion current can be considered proportional to the desorption rate.

The possible existence of mass transfer resistances was assessed by calculating the Thiele modulus at the conditions of maximum desorption rate. Values of the specific surface area (S_g), the pore volume (V_g), average pore radius (r_p) and the particle diameter (d_p) of the powdery fumed silicas used in this work have been previously reported in several works by Gun'ko *et al.*:[37,38] $S_g = 294{-}300\,m^2\,g^{-1}$, $V_g = 0.44{-}0.57\,cm^3\,g^{-1}$, $r_p = 3.0{-}3.2\,nm$, $d_p = 15\,\mu m$). Due to the low pressure used in the experiment only wall-molecule collisions were assumed to be present and the diffusivity was considered to be of the Knudsen type. The classical formulas for the Thiele modulus (h) and the Knudsen diffusivity (D_K) were taken from Carberry's textbook.[39] The effective diffusivity inside the pores was calculated as the product of D_K by the particle porosity ($\varepsilon = 0.565$), disregarding the effect of tortuosity and restriction factors. The kinetic constant in Thiele's formula was taken equal to k_d after assuming that desorption is the rate-limiting step in the mechanism. Then at the temperature of maximum rate of desorption of coumarins from the silica surface ($\approx$700 K) the values found for the relevant parameters are: $D_K = 5 \times 10^{-4}\,cm^2\,s^{-1}$; $k_d = 0.0045\,s^{-1}$; $h = 0.0057$. As it can be seen the reacting system is in the kinetic regime ($h \ll 0.4$), i.e. mass diffusional constraints are absent.

Temperature-programed desorption mass spectrometry and kinetic parameters

The nonisothermal parameters of desorption (thermal decomposition) and chemical reactions in the condensed phase and on silica surface were calculated using the personally designed computer program. This program enables the calculation of various nonisothermal kinetic parameters of the reactions in the condensed phase and on the surface of highly dispersed oxides, such as the order of the reaction (n), the pre-exponential factor (ν), activation energy ($E^{\neq}$), and activation entropy ($dS^{\neq}$) from TPD-MS data. The nonisothermal parameters were calculated only for well-resolved peaks, the peaks for which the form and position on the temperature scale were reproduced in several experiments. These nonisothermal parameters were calculated from the traces of well-resolved peaks for which form and position on the temperature scale were repeated in several experiments.

The procedure of obtaining kinetic parameters from TPD-MS data has been extensively described in a number of works and reviews.[6–12,29,40–42] The Arrhenius plot method was used in this work. This method is conveniently described in full detail elsewhere[29,42] but a short description is written in the following paragraphs.

The process of desorption from solid surface can be described by kinetic Eqn (1), and the desorption rate constant k_d by Arrhenius

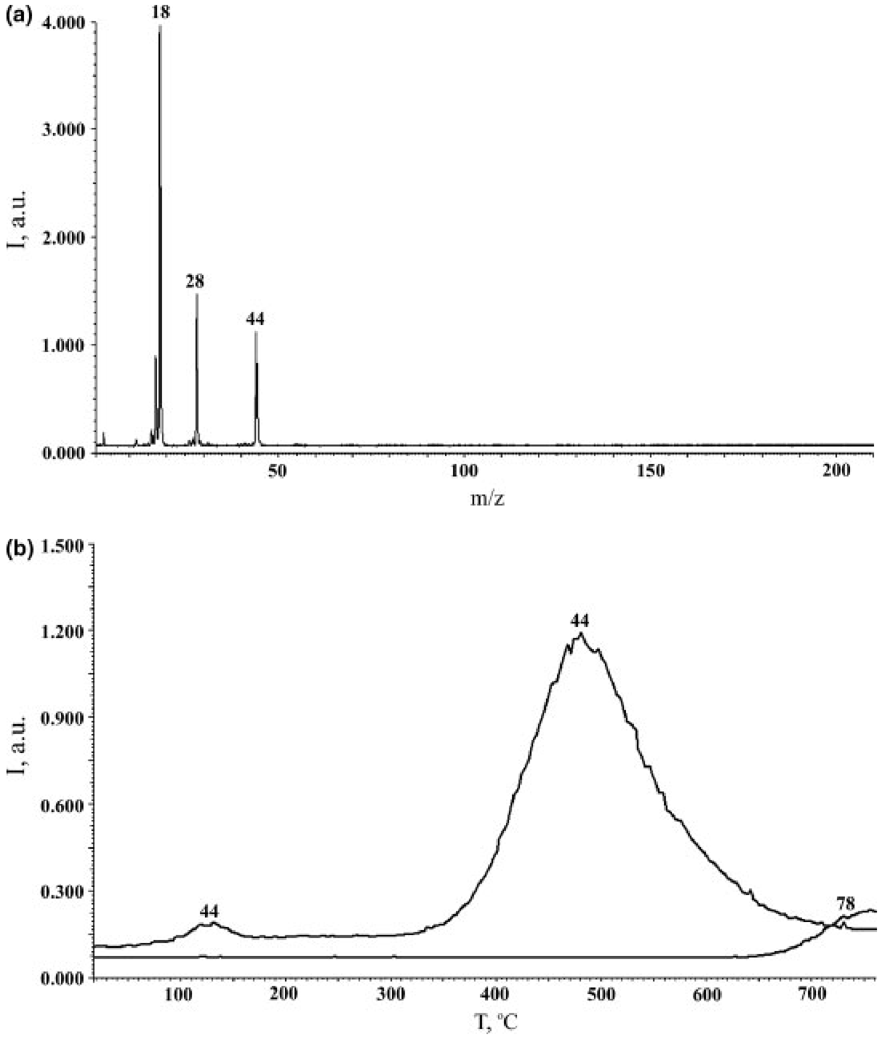

Figure 1. Mass spectrum at 470 °C (a) and thermal desorption traces of the ions with $m/z = 44$ and 78 (b), corresponding to the decomposition of silica-supported umbelliferone (1) (0.3 mmol g^{-1}).

Eqn (2). Substitution of Eqn (1) into Eqn (2) yields Eqn (3):

$$d\theta/dt = -k_d\,\theta^n \tag{1}$$

$$k_d = \nu \exp(-E^{\neq}/RT) \tag{2}$$

$$d\theta/dt = \theta^n\,\nu\,\exp(-E^{\neq}/RT) \tag{3}$$

where θ is the surface coverage ($\theta = 0{-}1$), t is time (s), k_d is the desorption rate constant, n is the order of the reaction, ν is the pre-exponential factor (1/s), $E^{\neq}$ is the activation energy for desorption (J/mol), R is the universal gas constant (J/mol K) and T is temperature (K).

If the $E^{\neq}$ and ν rates do not depend on the temperature or surface concentration, the desorption order can be obtained by plotting $\ln(\theta^{-n}\,d\theta/dt)$ as a function of $1/RT$. From this plot the value of the reaction order, n, can be obtained, which is equal to either 1 or 2. The true value is the one that gives a linear dependence with a slope $-E^{\neq}$ ($tg\alpha = -E^{\neq}$) and with a high correlation coefficient ($R^2 = 0.95{-}1$). The substitution of $E^{\neq}$ into Eqn (3) permits obtaining ν, for $\ln(\nu) = E^{\neq}/RT$ at $\ln(k_d) = 0$.

The value of the entropy of activation $dS^{\neq}$ can be obtained with Eqn (4):

$$dS^{\neq} = k_b\,N_A\,\ln(h\,\nu/k_b\,T_{max}) \tag{4}$$

where k_b is Boltzmann's constant, N_A is Avogadro's constant, h is Planck's constant and T_{max} is the temperature of the maximum desorption rate.

Results and Discussion

The study of coumarins (**1–7**) in bulk condensed form has shown that in this state they possess high thermal stability. When heated in a vacuum they sublimate and form a thin layer over the cold areas of the mass spectrometer ampoule. For this reason, no mass spectra of bulk coumarins could be obtained in the TPD-MS experiments. In order to obtain such spectra, the direct injection or field desorption methods should be used.

The thermolysis data of the silica-supported coumarins (**1–7**) showed the presence of a molecular ion only in the case of the mass spectrum of the methoxy-derivative **4**. The other silica-supported coumarins were seemingly subjected to thermal degradation because their mass spectra lacked the molecular ion in the whole scanned temperature range.

The first step of the thermal decomposition of the silica-supported coumarins (**1–3**) and their heterocyclic derivatives with free hydroxyl groups (**5–7**) is decarboxylation. The TPD traces of

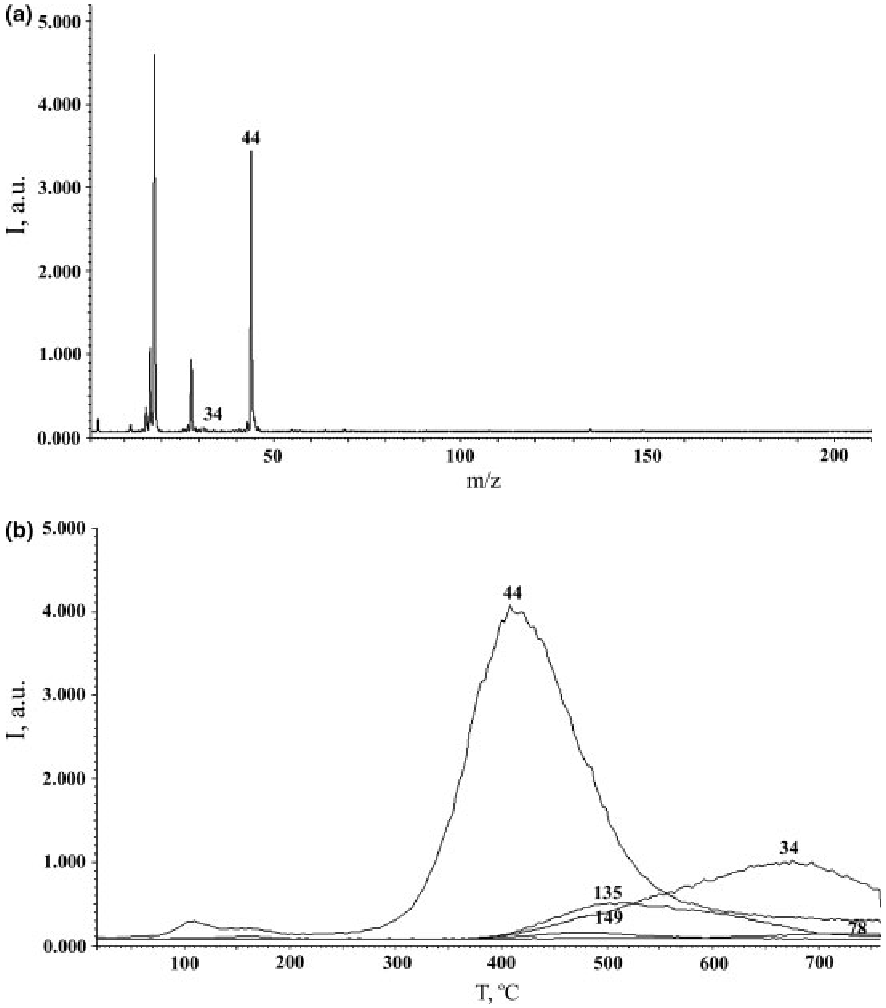

Figure 2. Mass spectrum at 391 °C (a) and thermal desorption traces of the ions with $m/z = 44$, 34, 78, 135 and 149 (b), corresponding to the thermal decomposition of silica-supported 3-(2-benzothiazol)-8-hydroxycoumarine (**6**) (0.4 mmol g^{-1}).

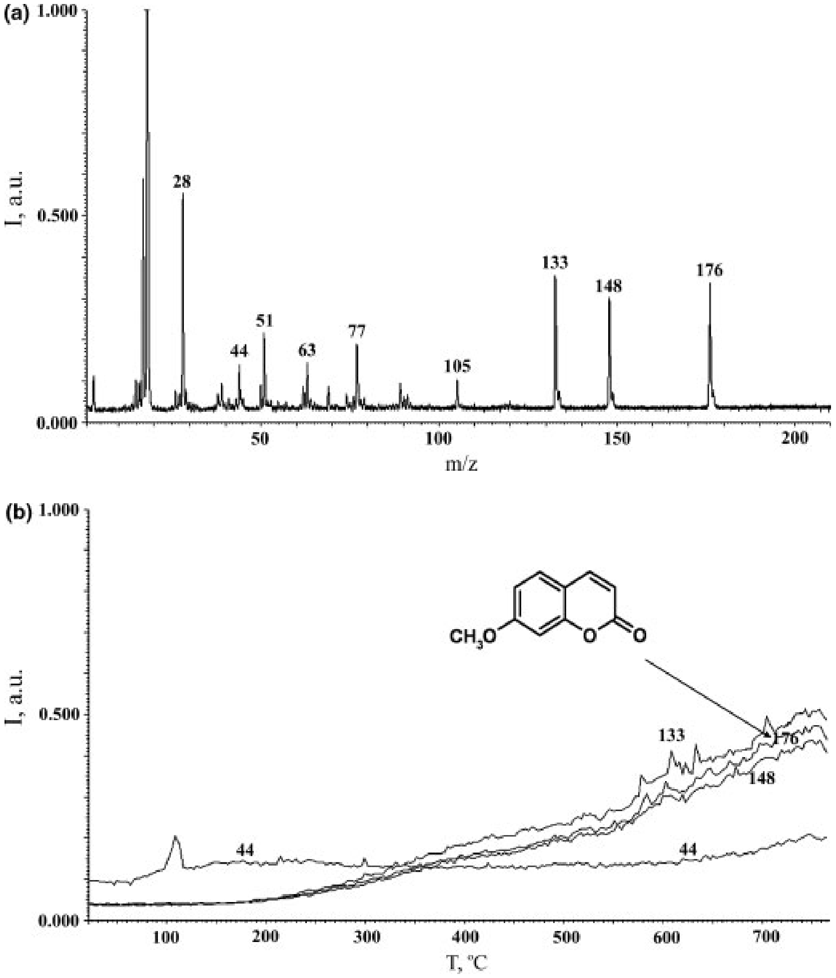

Figure 3. Mass spectrum at 350 °C (a) and thermal desorption traces of the ions with $m/z = 176$, 148 and 133 (b), corresponding to the desorption of silica-supported 7-methoxycoumarin (**4**) (0.3 mmol g^{-1}).

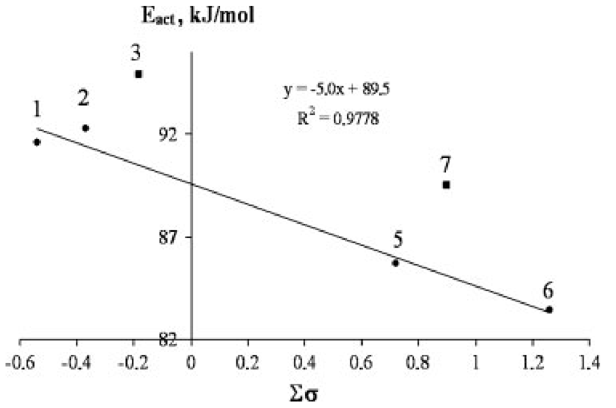

Figure 4. Correlation between the activation energy of decarboxylation of silica-supported coumarins and the constants of the coumarin substituents.

the ion with m/z 44 (CO_2) have an identical shape and their maxima occur at the same temperature (Figs 1 and 2).

Unlike **1–3** and **5–7** coumarins, the CO_2 TPD trace of 7-methoxy-coumarin (**4**) has no distinguishable peaks above 100 °C (Fig. 3). 7-methoxy-coumarin sublimates easily from the silica surface. The other spectra indicate that at temperatures higher than 200 °C, a molecular ion with $m/z = 176$ appears along with its rearrangement counterparts of $m/z = 148$, 133 and 105.[43] These are formed in the ion source of the mass spectrometer under the influence of electrons (Scheme 1).

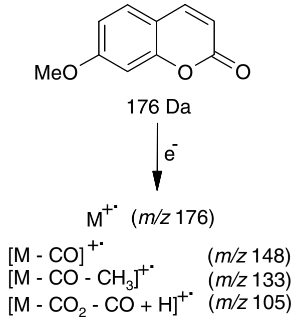

Scheme 1. EI mass fragmentation of 7-methoxy-coumarin (**4**).

This great difference in surface thermolysis patterns is caused by the change of of the –OH group to a $-OCH_3$ group. The presence and number of adsorbate OH groups play a crucial role in the adsorption over polar silica surfaces. Coumarins could be chemisorbed over silica in several ways and the a priori two most feasible are depicted in Scheme 2(a) and (b). The transition from

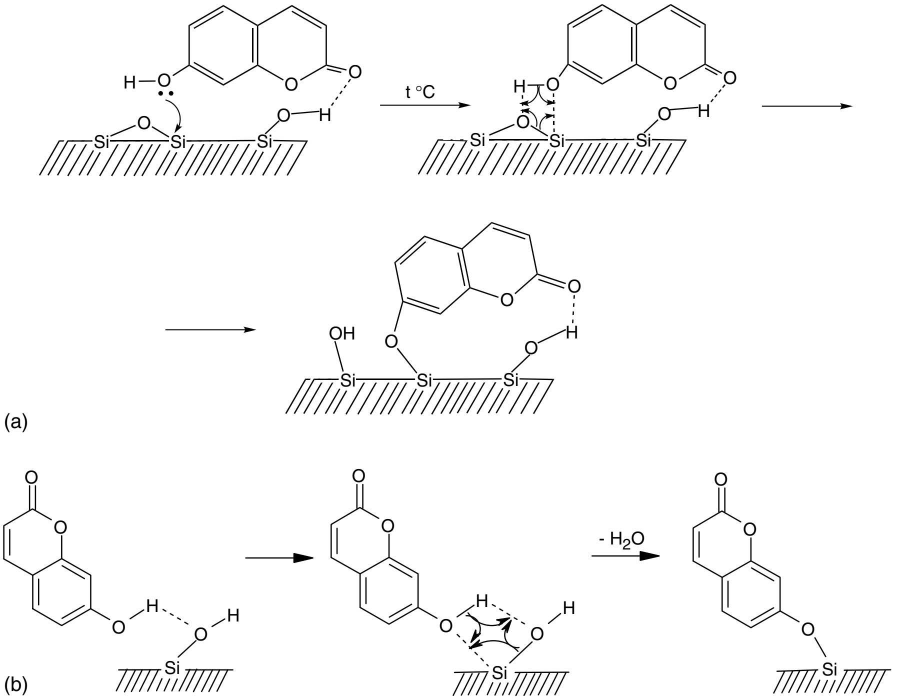

Scheme 2. (a) The chemisorption and subsequent protonation of oxygen in pyran-cycle carbonyls of 7-hydroxy-coumarin (1). (b) The chemisorption of 7-hydroxy-coumarin (1) on the surface silanol group.

physical adsorption to chemisorption would occur by hydroxyl-silanol condensation and water evolution during the heating of the sample ampoule in the TPD test.

The chemisorption and subsequent protonation of oxygen in pyran-cycle carbonyls or of nitrogen in thiazole and benzothiazole substituents would occur by proton donation from a silanol group. This protonation produces a redistribution of the electron density of coumarins. As a result, coumarin is degraded during the temperature increase of the TPD test. The weakest bonds are broken and carbon dioxide is formed. This is not seen in the case of the TPD test of bulk coumarin. For this reason, hydroxylated coumarins cannot desorb from the surface in their molecular form while methoxylated ones (**4**) can.

The kinetic parameters of the first- and second-order decarboxylation reaction were calculated (Table 1). The results indicate that the reaction is well described by a first-order model because in this case the correlation coefficient is the highest. The pre-exponential factors of all the seven samples studied were similar and had the same magnitude order, $\nu_{\text{average}} = 1.47 \cdot 10^4\ \text{s}^{-1}$. This is an indication that the structure of the transient state of the decarboxylation reaction for this series of coumarins is the same. In this case, the isoentropic series is studied. If we define $T_{\max}$ as the temperature at which the decarboxylation rate is maximum, we can see that $T_{\max}$ spans a range of about 100 °C for the set of coumarins and has the following order: **3**: 502 > **1**: 481 > **2**: 475 > **7**:458 > **5**:427 > **6**:408 °C. Decarboxylation rates and $T_{\max}$ seem therefore to be the features most affected by the presence of different substituents in the coumarin molecule. The lowest values of $T_{\max}$ are displayed by the heterocyclic coumarin derivatives (**5** and **6**). However a regular change in activation energy is not found in this studied series. This is because the energy of activation was calculated for the entire maximum, and the rated value of E_{act} was greatly influenced by the form of the front or back edges. For this reason, the energy of activation was calculated according to approximate formula:[40–42]

$$E^{\neq} = RT_{\max} \ln(B \ \ln B),\ \text{where}\ (B = n\ \nu\ T_{\max}\ C_{\max}{}^{n-1}/b) \qquad (5)$$

In this formula $\nu = \nu_{\text{average}} = 1.47 \cdot 10^4\ \text{s}^{-1}$, n is the reaction order, $C_{\max}{}^{n-1}$ is the concentration of the adsorbate at $T_{\max}$ and b is the value of the sample heating rate. The thus calculated value $E^{\neq}$ has only a slight dependence on the B parameter.[40] It has been shown in the work of Redhead[40] that the logarithmic dependence of the activation energy on ν helps to decrease the error sensitivity of the analysis results. Thus reliable estimates of the activation energy can be obtained. For this reason for the first-order model and $\nu_{\text{average}} = 1.47 \times 10^4\ \text{s}^{-1}$, the following approximate correlation can be used:

$$E^{\neq} = 15\ RT_{\max} \qquad (6)$$

The calculation of the activation energy with this approximate formula made it possible to obtain a linear correlation ($R^2 = 0.978$) between the sigma constants ($\Sigma\sigma$) of the coumarin substituents and the activation energies of decarboxylation of coumarins **1**, **2**, **5** and **6** (Fig. 4). The deviation from the correlation displayed by coumarins **3** and **7** is attributed to the ortho-effect of the substituents. The sigma constants were obtained from the experimental data by calculating the effect of the substituents on the value of pK for the model series of corresponding coumarin acids. Calculations were made with the Analytical Data Handling and Physicochemical Prediction modules of the ACD Labs Software package.

The observed linear correlation shows that the LFER principle applies to the free energy of reaction and the activation energy of the correlated reaction series. The decrease of the activation energy at increasing values of the electron-seeking force of the substituents indicates that the electron density in the transition state grows, i.e. the reaction parameter ρ has a positive value.

Table 1. Kinetic parameters of the chemical reactions of silica-supported coumarins

Sample, amount on silica surface	Reaction product	$T_{\mathbf{max}}$, °C	m/z	n	$E^{\neq}$, kJ·mol^{-1}	ν, s^{-1} ($n = 1$); l·mol^{-1} s^{-1} ($n = 2$)	$dS^{\neq}$, cal·K^{-1}·mol^{-1}	R^2
SiO_2								
Coumarin **1**, 0.3 mmol g^{-1}	CO_2	481	44	1	99	1.36×10^4	−41.6	0.952
			44	2	177	8.49×10^9	−14.9	0.944
Coumarin **2**, 0.6 mmol g^{-1}	CO_2	475	44	1	100	2.10×10^4	−40.6	0.959
			44	2	197	3.25×10^{11}	−7.7	0.949
	Phenylacetylene	617	102	1	166	1.03×10^7	−28.6	0.932
Coumarin **3**, 0.3 mmol g^{-1}	CO_2	502	44	1	99	1.21×10^4	−41.8	0.952
				2	163	1.37×10^9	−18.6	0.848
Coumarin **5**, 0.4 mmol g^{-1}	CO_2	427	44	1	92	1.88×10^4	−40.6	0.955
				2	160	3.04×10^9	−16.8	0.888
	4-methylthiazole	457	99	1	96	1.33×10^4	−41.4	0.954
	4H-3-methyl-1,4-thiazine	437	113	1	153	5.24×10^{10}	−20.4	0.969
Coumarin **6**, 0.4 mmol g^{-1}	CO_2	408	44	1	91	1.50×10^4	−38.6	0.950
				2	175	1.12×10^{11}	−9.6	0.927
	Benzothiazole	512	135	1	104	1.60×10^4	−41.1	0.953
	Benzo-4H-1,4-thiazine	465	149	1	126	1.55×10^6	−32	0.941
Coumarin **7**, 0.3 mmol g^{-1}	CO_2	458	44	1	99	2.11×10^4	−40.5	0.96
	4-methyl-thiazole	487	99	1	113	1.66×10^5	−36.5	0.980
	4H-3-methyl-1,4-thiazine	449	113	1	137	2.5×10^7	−26.4	0.960
4-Methylthiazole, 0.3 mmol g^{-1}	4H-3-methyl-1,4-thiazine	109	113	1	63	2.57×10^6	−29.6	0.954
CeO_2/SiO_2								
Coumarin **7**, 0.3 mmol g^{-1}	CO_2	420	44	1	90	1.75×10^4	−40.6	0.950
	4-methylthiazole	433	99	1	100	9.18×10^4	−37.5	0.968
	4H-3-methyl-1,4-thiazine	406	113	1	109	1.17×10^6	−32.5	0.977
TiO_2/SiO_2								
Coumarin **7**, 0.3 mmol g^{-1}	CO_2	440	44	1	87[a]	$\sim 10^4$	–	–
	4H-3-methyl-1,4-thiazine	407	113	1	113[b]	$\sim 10^6$	–	–
Al_2O_3/SiO_2								
Coumarin **7**, 0.3 mmol g^{-1}	CO_2	350	44	1	76[a]	$\sim 10^4$	–	–
		510	44	1	96[a]	$\sim 10^4$	–	–
	4H-3-methyl-1,4-thiazine	370	113	1	107[b]	$\sim 10^6$	–	–
		479	113	1	125[b]	$\sim 10^6$	–	–

[a] The activation energy was calculated according to approximation formula $E^{\neq} = 15 \cdot RT_{\max}$.
[b] The activation energy was calculated according to approximation formula $E^{\neq} = 20 \cdot RT_{\max}$.

It must also be remarked that as the correlations obtained from the LFER principle are empirical it is not necessary to know the exact absolute values of the activation energy.[15] For example, sometimes only some information about the order of magnitude for the reaction parameter ρ is enough for clarifying the reaction mechanism. These minimum and approximate pieces of information are usually the answers to the questions:[15] Is the constant ρ positive or negative? Is its numerical value large or small? Are there any appreciable aberrations from the curve linearity?[15]

After CO_2 is detached, the coumarin fragments that remain adsorbed seemingly polymerize on the silica surface. Upon further heating above 500 °C some coumarin samples (**1–3, 5–7**) release ions with $m/z = 102$ and 78. Coumarin **2** also displays a TPD trace of $m/z = 128$ (Fig. 5) indicating[43] that naphthalene (128 Da), phenylacetylene (102 Da) and benzene (78 Da) are released during the degradation of the polymer. The traces of thermal desorption of these compounds are those with $m/z = 128$, 102 and 78. These traces have well-resolved peaks (Fig. 5) that can be analyzed to obtain the corresponding kinetic parameters of desorption. Table 1 contains the values of these parameters for the case of the formation of phenylacetylene.

From the previous analysis of the TPD-MS data, the thermal transformations of silica-supported coumarins **1–3** can be described by a common mechanism exemplified in Scheme 3 for the case of coumarin **2**.

Coumarins **5–7** are found to undergo further thermolysis stages (Figs 6 and 7) that correspond to the thermal transformations of the heterocyclic substituent. Coumarin **5** is found to have TPD peaks in the traces of $m/z = 113$, 99 and 71 (Fig. 6). Coumarin **6** has similar peaks at $m/z = 149$, 135 and 108 (Fig. 7). According to the AIST database,[43] the lines in the mass spectra shown in Figs 6 and 7 correspond to 4-methylthiazole ($m/z = 99$) and benzothiazole ($m/z = 135$). Most likely, the second stage of thermolysis of coumarins **5** and **6** occurs with emission of molecular 4-methylthiazole (Scheme 4) and benzothiazole (Scheme 5), respectively.

It is interesting to note that in the case of coumarins with heterocyclic substituents (**5–7**) the desorption products have a molecular mass that differs from that of the heterocyclic substituent by 14 amu. These are the products with $m/z = 113$ (**5** and **7**) and $m/z = 149$ (**6**). The maximum in the TPD trace of the ion with $m/z = 113$ can be explained by the emission of

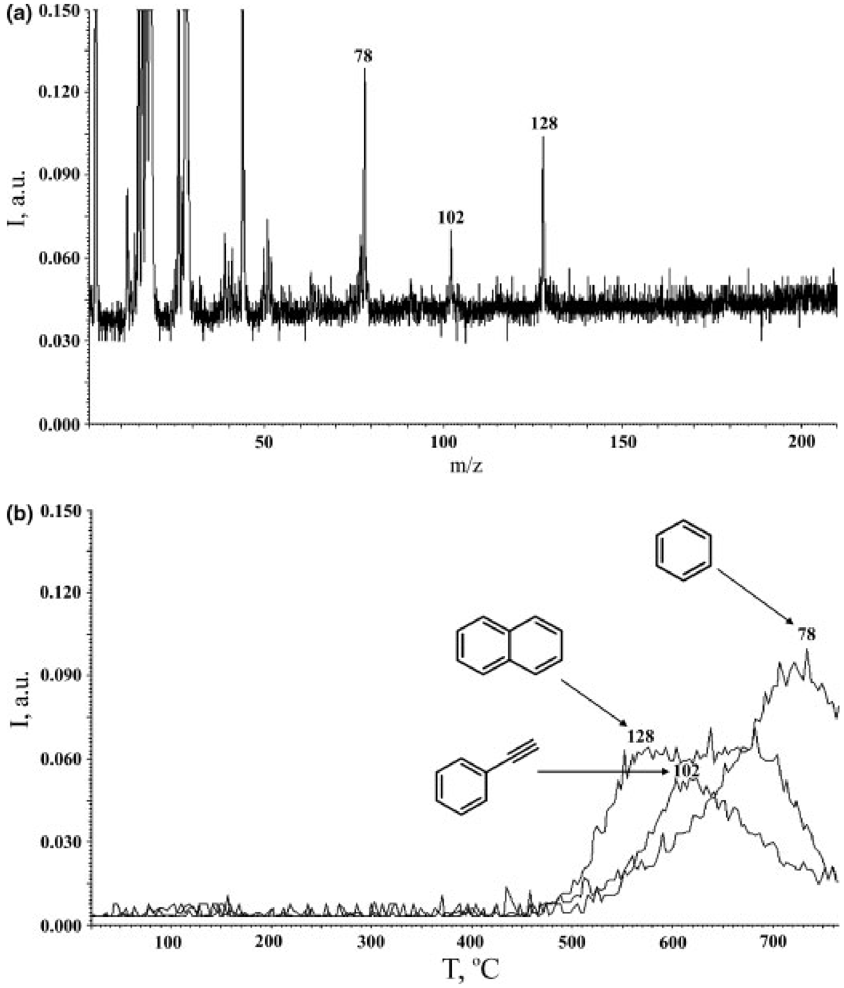

Figure 5. Mass spectrum at 704 °C (a) and thermal desorption traces of the ions with m/z = 128, 102 and 78 (b), corresponding to the thermal decomposition of silica-supported 4 methyl-7-hydroxycoumarin (**2**) (0.6 mmol g^{-1}).

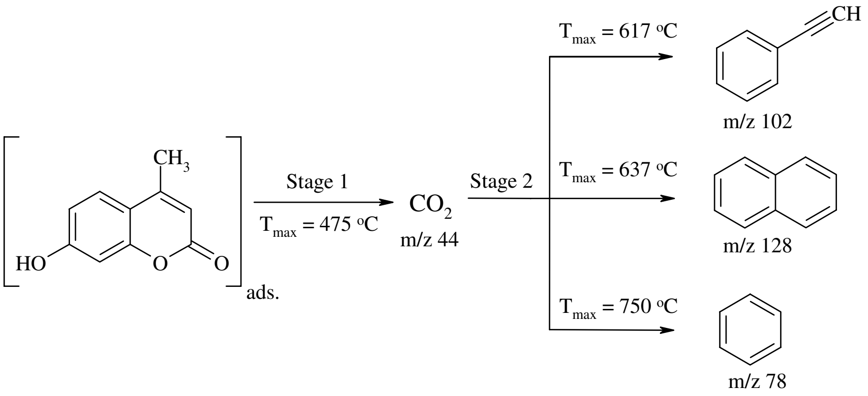

Scheme 3. The thermal decomposition of silica supported 4-methyl-7-hydroxycoumarin (**2**).

molecular 4H-3-methyl-1,4-thiazine (113 Da). In the case of the ion with m/z = 149, the peak can be attributed to the release of benzo-4l-1,4-thiazine (149 Da) (Schemes 4 and 5). Thiazine formation is thus likely the result of the rearrangements of thiazole and benzothiazole substituents on the silica surface.

The complex chemical reactions involving the heterocyclic substituents (4-methylthiazole and benzothiazole) and occurring on the silica surface at high temperatures are associated to the peaks in the traces of ions with m/z = 32 and 34 that correspond to the formation of H_2S (Figs 2, 6 and 7).

Additional TPD-MS tests of silica samples impregnated with 4-methylthiazole show that the mass spectrum at 105 °C has a line with m/z = 113. This ion has a TPD trace with a maximum at T_{max} = 110 °C (Fig. 8; Table 1). The mass spectrum of bulk 4-methylthiazole, obtained by flooding the sample ampoule with its vapors, does not contain the line of m/z = 113. These

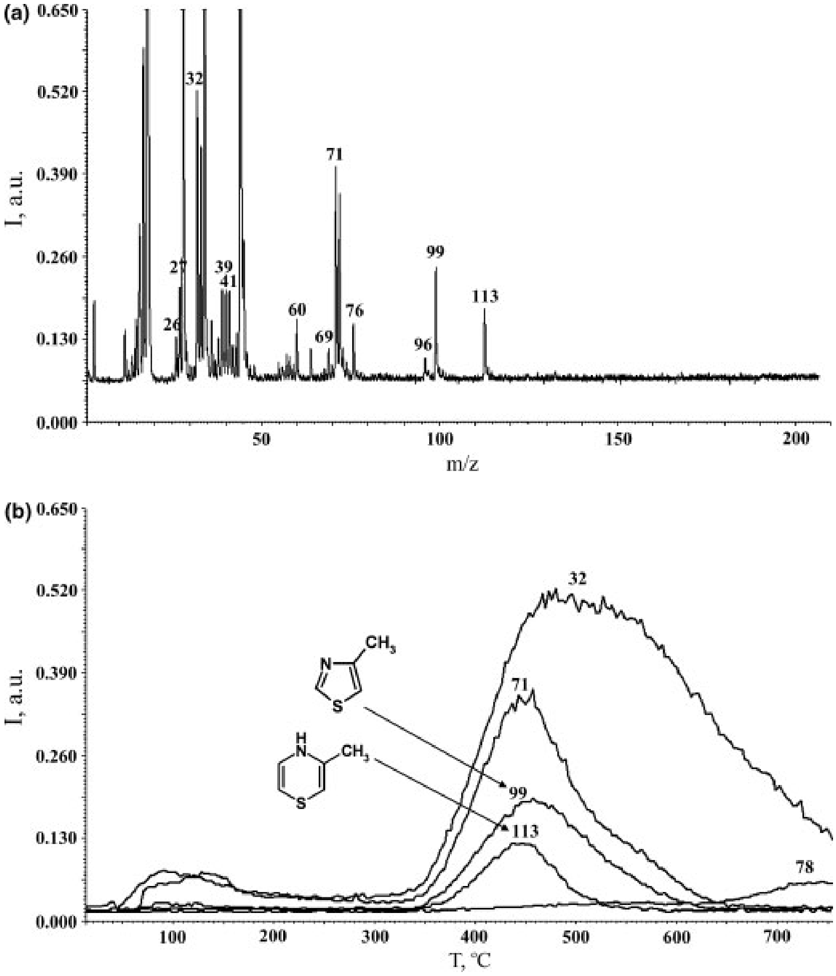

Figure 6. Mass spectrum at 447 °C (a) and thermal desorption traces of the ions with $m/z = 32, 71, 78, 99$ and 113 (b), corresponding to the decomposition of silica-supported 3-(4-methyl-1,3-thiazol-2-yl)-7-hydroxycoumarin (**5**) (0.4 mmol g^{-1}).

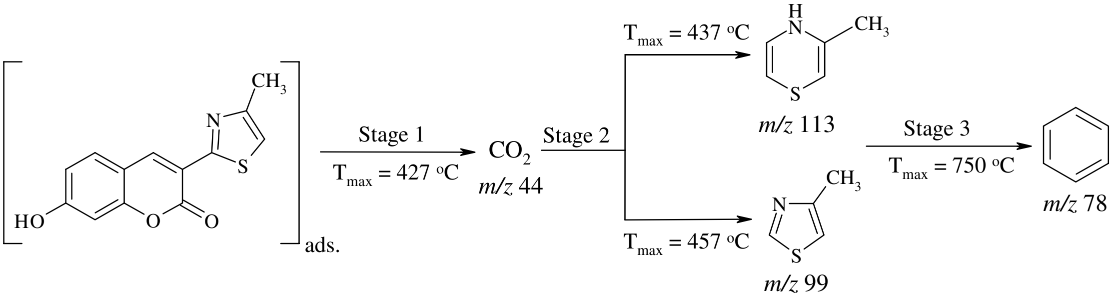

Scheme 4. The decomposition of silica supported 3-(4-methyl-2-thiazole)-7-hydroxycoumarin (**5**).

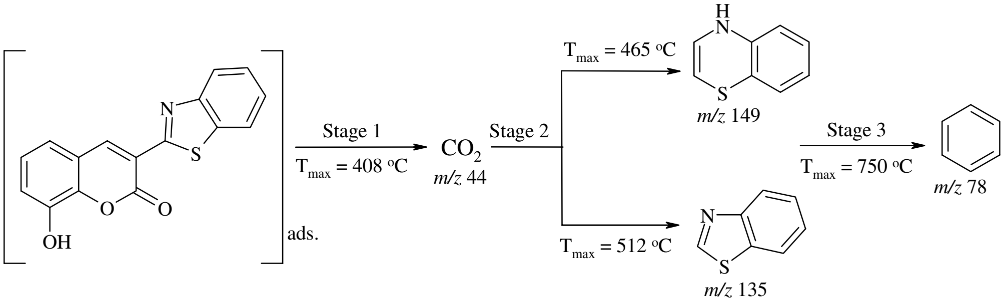

Scheme 5. The thermal decomposition of silica supported 3-(2-benzothiazole)-8-hydroxycoumarine (**6**).

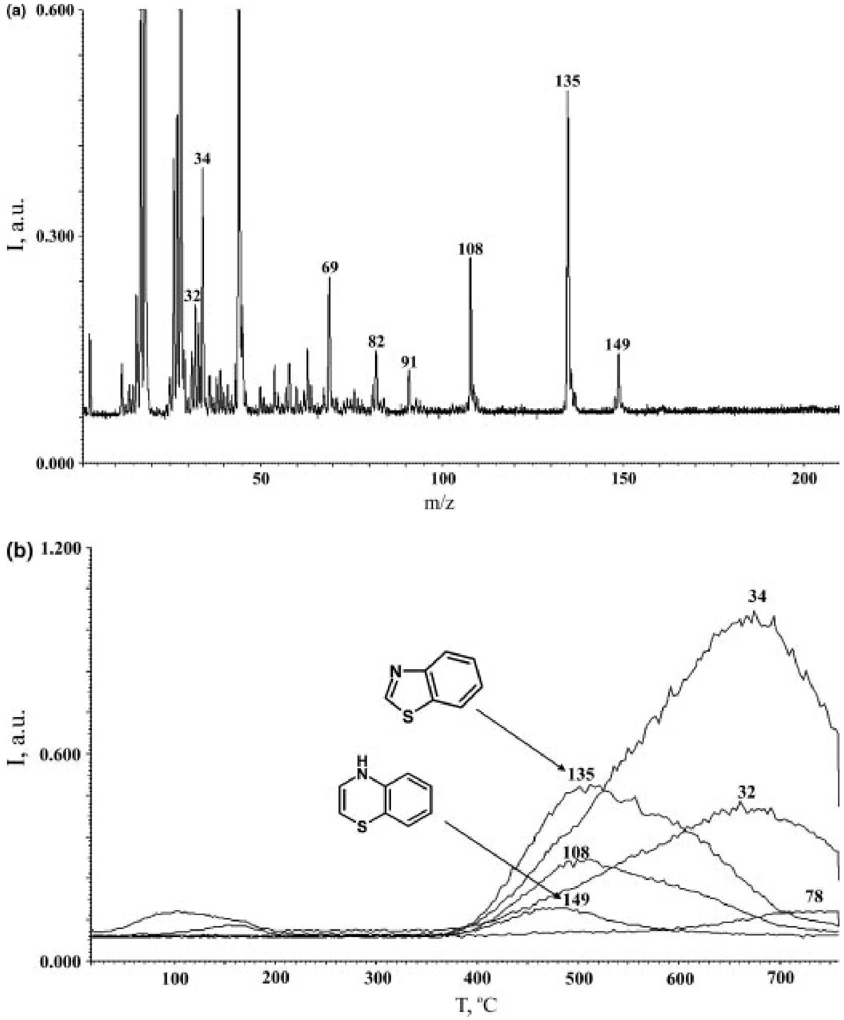

Figure 7. Mass spectrum at 518 °C (a) and thermal desorption traces of the ions with $m/z = 149, 135, 108, 78, 34$ and 32 (b), corresponding to the thermal decomposition of silica-supported 3-(1,3-benzothiazol-2-yl)-8-hydroxycoumarin (**6**) (0.4 mmol g^{-1}).

data confirm the presence of rearrangements of isolated 4-methylthiazole when grafted on the silica surface though the exact mechanism has not been yet elucidated.

The TPD traces of the ions with $m/z = 99$ and 113 corresponding to the thermolysis of coumarin **5** and those of $m/z = 135$ and 149 corresponding to coumarin **6** have no overlapping peak temperatures (Figs 6 and 7). This indicates that two different surface chemical processes are occurring in each case. The peaks of release of molecular heterocyclic substituents are wider and shifted to higher temperatures as compared to those corresponding to the release of products of rearrangement.

The maximum rate of 4-methylthiazole formation on silica occurs at $T_{max} = 457\,^{\circ}C$. This is shifted to lower temperatures by 55 °C in the case of benzothiazole ($T_{max} = 502\,^{\circ}C$). It can be seen that the ion with $m/z = 113$ has a maximum release rate at a lower temperature ($T_{max} = 437\,^{\circ}C$) than 4-methylthiazole. The same occurs with the ion of $m/z = 149$ in comparison to benzothiazole ($T_{max} = 465\,^{\circ}C$). This means that 4-methylthiazole and benzothiazole desorb from the surface at higher temperatures than the products of surface rearrangement.

The thiazole–thiazine rearrangement occurred during the pyrolysis of all the thiazole heterocycles, i.e. pure thiazole and substituted coumarins. Kinetic parameters (n, $E^{\neq}$, ν, $dS^{\neq}$) of the silica-assisted reaction of thiazine formation were also calculated for the CeO_2/SiO_2, Al_2O_3/SiO_2 and TiO_2/SiO_2 systems (Fig. 9; Table 1). The activation energy of the thiazole–thiazine rearrangement decreased in the order: $SiO_2 > CeO_2/SiO_2 \approx TiO_2/SiO_2 > Al_2O_3/SiO_2$. It is interesting to note that thermodesorption curve for m/z 113 have two maximums ($T_{max} = 370\,^{\circ}C$ and $T_{max} = 510\,^{\circ}C$) during thermolysis on the surface of Al_2O_3/SiO_2. Perhaps this phenomenon could be attributed to contribution of Lewis acid centers on thermodestruction process.

Formation of CO_2 on surface of mixed oxides also occurs at lower temperatures with respect to pure fumed silica (Fig. 10; Table 1). Two maximums on the stage of carbon dioxide formation are observed on the surface of Al_2O_3/SiO_2.

Conclusions

It has been found that free hydroxyls groups in positions 7 and 8 of the coumarin nucleus play a crucial role in the chemisorption of these molecules to the silica surface. Thermolysis stages were found to be related to certain structural elements of natural and

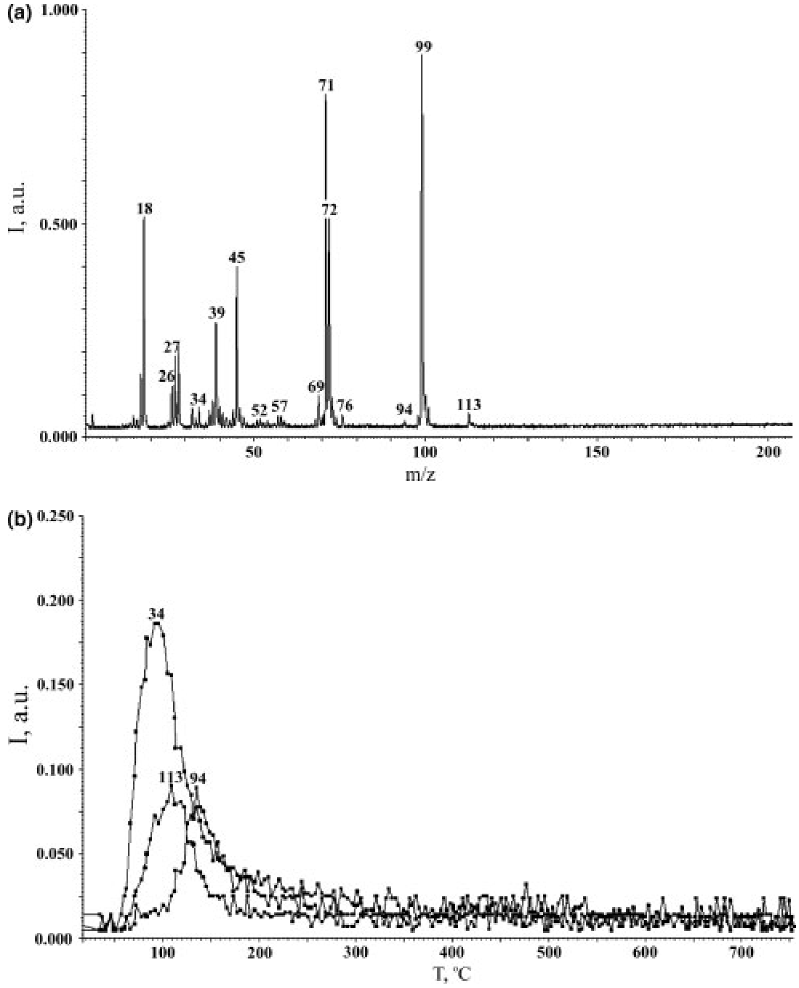

Figure 8. Mass spectrum at 105 °C (a) and TPD-MS traces of a silica sample impregnated with 4-methylthiazole (b).

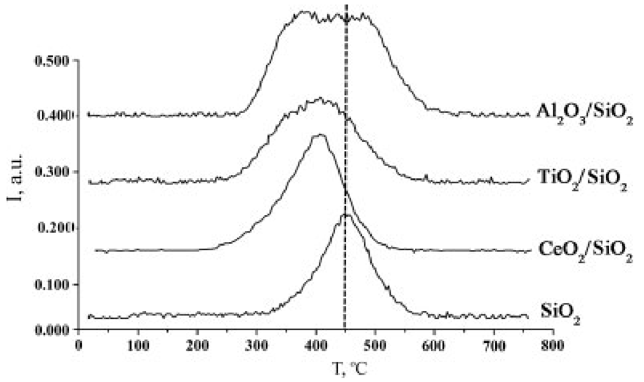

Figure 9. Thermal desorption traces of the ions with $m/z = 113$ corresponding to the thermal decomposition of pure silica and mixed oxide-supported 7-hydroxy-3-(4-methyl-1,3-thiazol-2-yl)-8-(pyrrolidin-1-ylmethyl)coumarine (**7**).

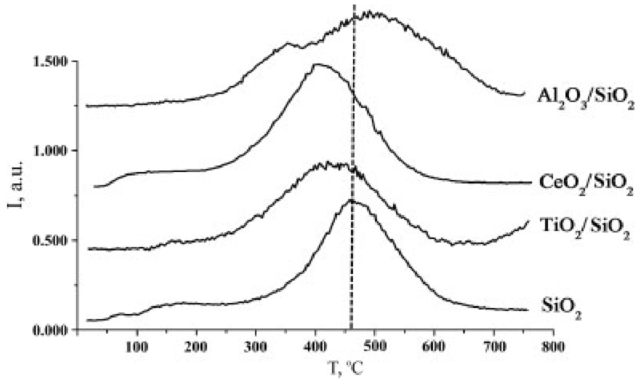

Figure 10. Thermal desorption traces of the ions with $m/z = 44$ corresponding to the thermal decomposition of pure silica and mixed oxide-supported 7-hydroxy-3-(4-methyl-1,3-thiazol-2-yl)-8-(pyrrolidin-1-ylmethyl)coumarine (**7**).

modified coumarins: the coumarin nucleus, the thiazole and the benzothiazole substituents.

The thermal degradation of the studied silica-supported coumarins starts with the detachment of a CO_2 molecule and the further release of molecular benzene, naphthalene and phenylacetylene at temperatures over 500 °C.

A linear correlation between the activation energy for decarboxylation of the silica-supported coumarins and the sigma constants ($\Sigma\sigma$) of their substituents was obtained.

Heterocyclic coumarine derivatives are found to have additional thermolysis stages that encompass the release of molecular heterocyclic compounds, particularly 4-methylthiazole and benzothiazole. Rearrangements in the adsorbed state proceeded through a 'thiazole–thiazine' ring expansion.

The activation energies of the thiazole–thiazine rearrangement and reaction of CO_2 formation decreased in the order: $SiO_2 > CeO_2/SiO_2 \approx TiO_2/SiO_2 > Al_2O_3/SiO_2$.

Acknowledgements

The authors thank Prof. V.M. Gun'ko and Dr V.I. Zarko (Chuiko Institute of Surface Chemistry, Kyiv) for some oxide samples.

References

[1] F. Hillenkamp, M. Karas. Matrix-assisted laser desorption/ionisation, an experience. *Int. J. Mass Spectrom.* **2000**, *200*, 71.
[2] K. Breuker, R. Knochenmuss, R. Zenobi. Proton transfer reactions of matrix-assisted laser desorption/ionization matrix monomers and dimers. *J. Am. Soc. Mass Spectrom.* **1999**, *10*, 1111.
[3] R. Zenobi, R. Knochenmuss. Ion formation in MALDI mass spectrometry. *Mass Spectrom. Rev.* **1999**, *17*, 337.
[4] R. Knochenmuss, A. Stortelder, K. Breuker, R. Zenobi. Secondary ion-molecule reactions in matrix-assisted laser desorption/ionization. *J. Mass spectrom.* **2000**, *35*, 1237.
[5] S. Alimpiev, A. Grechnikov, J. Sunner, V. Karavanskii, Ya. Simanovsky, S. Zhabin, S. Nikiforov. On the role of defects and surface chemistry for surface-assisted laser desorption ionization from silicon. *J. Chem. Phys.* **2008**, *128*, 14711.
[6] R. J. Cvetanovic, Y. Amenomiya. A temperature programmed desorption technique for investigation of practical catalysts. *Catal. Rev.* **1972**, *6*, 21.
[7] J. A. Delgado, J. M. Gomez. Estimation of Adsorption Parameters From Temperature-Programed-Desorption Thermograms: Application to the Adsorption of Carbon Dioxide onto Na- and H-Mordenite. *Langmuir* **2005**, *21*, 9555.
[8] S. I. Nicholl, J. W. Talley. Development of thermal programmed desorption mass spectrometry methods for environmental applications. *Chemosphere* **2006**, *63*, 132.
[9] J. B. Miller, H. R. Siddiqui, S. M. Gates, J. N. Russell, J. T. Yates. Extraction of kinetic parameters in temperature programmed desorption: a comparison of methods. *J. Chem. Phys.* **1987**, *87*, 6725.
[10] S. I. Nicholl, J. W. Talley, S. Silliman. Model verification of thermal programmed desorption-mass spectrometry for estimation of release energy values for polycyclic aromatic hydrocarbons on mineral sorbents. *Environ. Toxicol. Chem.* **2004**, *23*, 2545.
[11] T. Panczyk, P. Szabelski. The influence of lateral interactions between adsorbed molecules on adsorption kinetics. A statistical rate theory approach. *J. Phys. Chem. B* **2003**, *107*, 5586.
[12] W. Rudzinski, T. Panczyk. Remarks on the current state of adsorption kinetic theories for heterogeneous solid surfaces: a comparison of the ART and the SRT approaches. *Langmuir* **2002**, *18*, 439.
[13] V. V. Brei, V. M. Gun'ko, V. V. Dudnik, A. A. Chuiko. Study of Kinetics and Mechanisms of Some Unimolecular Reactions on Silica Surfaces. *Langmuir* **1992**, *8*, 1968.
[14] V. M. Gun'ko, I. F. Mironyuk, V. I. Zarko, E. F. Voronin, V. V. Turov, E. M. Pakhlov, E. V. Goncharuk, Y. M. Nychiporuk, N. N. Vlasova, P. P. Gorbik, O. A. Mishchuk, A. A. Chuiko, T. V. Kulik, B. B. Palyanytsya, S. V. Pakhovchishin, J. Skubiszewska-Zięba, W. Janusz, R. Leboda. Morphology and surface properties of fumed silicas. *J. Colloid Interface Sci.* **2005**, *289*, 427.
[15] P. Sykes. *A Guidebook to Mechanism in Organic Chemistry*. Longman Scientific&Technical: London, **1986**.
[16] H. H. Jaffe. A Reexamination of the Hammett Equation. *Chem. Rev.* **1953**, *53*, 191.
[17] P. R. Wells. Linear Free Energy Relationships. *Chem. Rev.* **1963**, *63*, 171.
[18] P. R. Wells, *Linear Free Energy Relationships*. Academic Press: New York, **1968**.
[19] L. P. Hammet. Some Relations between Reaction Rates and Equilibrium Constants. *Chem. Rev.* **1935**, *17*, 125.
[20] L. P. Hammet. *Physical Organic Chemistry*, 2nd ed. McGraw-Hill: New York, **1970**.
[21] R. W. Taft. Polar and Steric Substituent Constants for Aliphatic and o-Benzoate Groups from Rates of Esterification and Hydrolysis of Esters. *J. Am. Chem. Soc.* **1952**, *74*, 3120.
[22] R. W. Taft, C. Grob. Separation of polar and resonance effects in the ionization of 4-substituted pyridinium ions. *J. Am. Chem. Soc.* **1974**, *96*, 1236.
[23] B. J. Bronsted. Die katalytische Zersetzung des Nitramids und ihre physikalisch-chemische Bedeutung. *Z. Phys. Chem.* **1924**, *108*, 185.
[24] M. Kraus. *Advances in Catalysis*, vol. 17. Academic Press: New York and London, **1967**, 75.
[25] V. P. Khylya, O. V. Shablykina, V. V. Ishchenko. *Selected Methods for Synthesis and Modification of Heterocycles*, vol. 2,V. G. Kartsev (Ed). IBS PRESS: Moscow, **2003**, 518 (in Russian).
[26] M. E. Perelson, Yu.N. Sheinker, A. A. Savina. *Spectra and Structures of Coumarins, Chromones and Xanthones*. Meditsina: Moscow, **1975**.
[27] *Medical Chemistry and Clinical Applications of Silica Dioxide*, A. A. Chuiko (ED). Naukova Dumka: Kyiv, **2003**, 416 (in Russian).
[28] T. V. Kulik, N. P. Galagan, V. K. Pogoreliy, V. A. Pokrovskiy, *Advances in Mass Spectrometry*, *Proceedings of the 15th International Mass Spectrometry Conference*, vol. 15,E. Gelpi (Ed). John Wiley&Sons: Chichester, **2001**, 491.
[29] V. A. Pokrovskiy, N. P. Galagan, T. V. Kulik. *Chemistry, Physics and Technology of Surface*, vol 4–6,O. O. Chuiko (Ed). Institute of Surface chemistry: Kyiv, **2001**, 332.
[30] T. V. Kulyk, V. V. Ischenko, B. B. Palyanytsya, V. P. Khylya, K. S. Kulyk, V. N. Barvinchenko, V. K. Pogorelyi. A study on interactions of coumarins and their heterocyclic derivatives with a surface of silica by desorption mass spectrometry method. *Mass-spectrometria* **2007**, *4*, 179 (in Russian).
[31] T. V. Kulik, N. A. Lipkovska, V. N. Barvinchenko, B. B. Palyanytsya, O. A. Kazakova, O. A. Dovbiy, V. K. Pogorelyi. Interactions between bioactive ferulic acid and fumed silica by UV-VIS spectroscopy FT-IR, TPD MS investigation and quantum chemical methods. *J. Colloid Interface Sci.* **2009**, *339*, 60.
[32] T. V. Kulik, V. N. Barvinchenko, B. B. Palyanytsya, O. V. Smirnova, V. K. Pogoreliy, A. A. Chuiko. A Desorption Mass Spectrometry Study of the Interaction of Cinnamic Acid with Silica Surface. *Russ. J. Phys. Chem.* **2007**, *81*, 83.
[33] M. V. Borysenko, K. S. Kulyk, M. V. Ignatovych, E. N. Poddenezhny, A. A. Boiko, A. O. Dobrodey. *Nanomaterials and Supramolecular Structures*, A. P. Shpak, P. P. Gorbyk (Eds). Springer: Dordrecht, The Netherlands, **2009**, 227.
[34] W. Rudzinski, T. Borowiecki, A. Dominko, T. Panczyk. A New Quantitative Interpretation of Temperature-Programmed Desorption Spectra from Heterogeneous Solid Surfaces, Based on Statistical Rate Theory of Interfacial Transport: The Effects of Simultaneous Readsorption. *Langmuir* **1999**, *15*, 6386.
[35] J. Park, R. T. Yang. Predicting Adsorption Isotherms of Low-Volatile Compounds by Temperature Programmed Desorption: Iodine on Carbon. *Langmuir* **2005**, *21*, 5055.
[36] J. Joly, A. Perrard. Determination of the Heat of Adsorption of Ammonia on Zeolites from Temperature-Programmed Desorption Experiments. *Langmuir* **2001**, *17*, 15.
[37] V. M. Gun'ko, J. Skubiszewska-Zięba, R. Leboda, V. I. Zarko. Fumed Silica Modified Due to Pyrolysis of Methylene Chloride. *Langmuir* **2000**, *16*, 374.
[38] J. P. Blitz, V. M. Gun'ko (Eds). *Surface Chemistry in Biomedical and Environmental Science*. Springer: Netherlands, Dordrecht, **2006**, 135.
[39] J. J. Carberry. *Chemical and Catalytic Reaction Engineering*. McGraw-Hill: New York, **1976**.
[40] P. A. Redhead. Thermal Desorption of Gases. *Vacuum* **1962**, *12*, 245.
[41] M. U. Kisliyk, V. V. Rozanov. Temperature-programmed desorption and temperature-programmed reaction - methods of studying of kinetics and mechanisms of catalytic processes. *Kinet. Katal.* **1995**, *36*, 89.
[42] D. P. Woodruff, T. A. Delchar. *Modern Techniques of Surface Science*. Cambridge University Press: London, **1986**.
[43] SDBSWeb. http://www.aist.go.jp/RIODB/SDBS/ (National Institute of Advanced Industrial Science and Technology, Last accessed: March 21, 2009).